Sensors and Actuators B 190 (2014) 120–126

Contents lists available at ScienceDirect

Sensors and Actuators B: Chemical

journal homepage: www.elsevier.com/locate/snb

Polyaniline/γ-Fe_2O_3 nanocomposite for room temperature LPG sensing

Tanushree Sen [a], Navinchandra G. Shimpi [a], Satyendra Mishra [a,*], Ramphal Sharma [b]

[a] University Institute of Chemical Technology, North Maharashtra University, Jalgaon 425001, Maharashtra, India
[b] Department of Physics, Dr. Babasaheb Ambedkar Marathwada University, Aurangabad 431004, Maharashtra, India

ARTICLE INFO

Article history:
Received 31 January 2013
Received in revised form 24 July 2013
Accepted 25 July 2013
Available online 31 August 2013

Keywords:
Polyaniline
γ-Fe_2O_3
Nanocomposite
LPG
Sensor

ABSTRACT

Polyaniline/γ-ferric oxide (PANi/γ-Fe_2O_3) nanocomposite films exhibited excellent sensing ability toward LPG at room temperature. The films were studied for their response to LPG at 50–200 ppm concentrations. The nanoscale morphology of the composites provided a large surface area for the adsorption of gas molecules, thus enhancing the gas sensitivity. The sensing mechanism pertains to a change in the depletion region of the p–n junction formed between PANi and γ-Fe_2O_3 as a result of electronic charge transfer between the gas molecules and the sensor. The maximum response was obtained for PANi/γ-Fe_2O_3 (3 wt%) nanocomposite for 200 ppm LPG. The response times of these sensors were found to be as low as 60 s.

1. Introduction

Nano-inorganic materials are used to improve the various properties of polymers like thermal [1], mechanical [2], weather [3], electrical [4], etc. Polyaniline (PANi) is one of the conducting polymers in which nanomaterials are used for their synergistic effect to improve electronic properties [5]. Among the nanosized metal oxides that have been the focus of research due to their potential application in electronic devices, maghemite (γ-Fe_2O_3) have attained prominence due to their magnetic, photocatalytic and electrochemical properties [6–8]. Complex structures of nanosized γ-Fe_2O_3 are being widely synthesized via various routes like hydrothermal [9], microwave [10], flame spray pyrolysis [11] and solvothermal [12]. Apte et al. [7] had also reported synthesis of α- and γ-Fe_2O_3 by combustion reaction of ferric nitrate, wherein necked structure morphologies were observed. These nanostructures of γ-Fe_2O_3 serve as sensing layers for gases, volatile organic compounds (VOCs) and other agents [13–15]. Room temperature sensing of hydrogen gas by flower-like nanostructures of hybrid ferric oxide has recently been reported by Agarwala et al. [16]. Fang et al. [17] have also reported ferric oxide quartz crystal microbalance (QCM) gas sensors for detection of dimethyl methylphosphonate. The high response of the sensor was due to the hollow structure of ferric oxide. Study regarding carbon monoxide detection by nanoflakes and nanowires of ferric oxide can also be found in the literature [18]. However, these sensors often show high response times which decrease only at high analyte concentration. High temperature detection of VOCs by ferric oxide/zinc oxide core–shell nanorods have been reported by Si et al. [19]. A particularly high response factor for petroleum was obtained by this sensor but at a temperature of 320 °C.

The one major drawback associated with sensing at high operating temperatures (~300–1000 °C) is that the sensor often suffers from instability and response variation as a result of structural changes in the sensing material caused by high temperature [20]. Additionally, high temperatures pose a threat during detection of combustible gases. Due to these limitations, intrinsically conducting polymers (ICPs) such as polyaniline (PANi), polypyrrole and polythiophenes are being increasingly used as sensing layers operating at room temperature. The ICPs have the advantage of higher sensitivity and enables safer detection of many inflammable gases and VOCs [21–23]. They have unique electronic properties due to the π-conjugation present in their backbones, and display improved characteristics over conventional sensors based on nanometal oxides. PANi, in particular, has been extensively used due to its ease of fabrication, high stability and electrical conductivity. Due to its singular redox properties, PANi has long been used in ammonia sensing [24–26], VOCs detection [27] and in QCM sensors [28]. Often, PANi is combined with nanostructured metals and metal oxides to induce selectivity in the material [27–29]. These nanocomposites of PANi with metal and metal oxides can be synthesized by various chemical and electrochemical methods, as

* Corresponding author. Tel.: +91 257 2258420; fax: +91 257 2258403.
E-mail addresses: profsm@rediffmail.com, profsm@live.com (S. Mishra).

0925-4005/$ – see front matter © 2013 Elsevier B.V. All rights reserved.
http://dx.doi.org/10.1016/j.snb.2013.07.091

reported in literature [29–31]. However, to the best of our knowledge, a PANi/γ-Fe_2O_3 system has not been studied for its sensitivity to liquefied petroleum gas (LPG) at room temperature so far. LPG is a flammable mixture of hydrocarbon gases (primarily propane and butane), which is used as a fuel in heating appliances and vehicles. It has a lower flammable limit (LFL) of 2% (20,000 ppm) in air. Therefore, upon any chance leakage, it poses a danger from possible explosion, and also suffocation since it displaces air causing a decrease in oxygen concentration [32].

In this paper we investigate the effectiveness of PANi/γ-Fe_2O_3 nanocomposite systems in sensing of LPG at room temperature. γ-Fe_2O_3 nanoparticles were synthesized sonochemically and deposited in situ into the PANi matrix. In addition, PANi and its nanocomposites were doped with a novel binary dopant. Conventional PANi doped with hydrochloric acid (HCl) gets de-doped in air over time, which limits their application as sensing layers. The binary dopant used in our experiments has shown to extend the life of PANi and its nanocomposites in doped form thereby increasing the material's stability in ambient conditions. Furthermore, the PANi/γ-Fe_2O_3 nanocomposites were found to be highly sensitive to LPG. These nanocomposite films have thus been used for detection of LPG at concentrations of 50–200 ppm, which is much lower than its LFL.

2. Experimental

2.1. Materials

Analytical grade aniline and ammonium persulphate (APS) were purchased from Fisher Scientific (Mumbai, India), sodium dodecyl sulphate (SDS), hydrochloric acid (HCl) and perchloric acid ($HClO_4$) from Himedia Laboratories Pvt. Ltd. (Mumbai, India) and N-methyl-2-pyrrolidone (NMP) from Merck (Mumbai, India). Anhydrous ferric chloride ($FeCl_3$) and sodium hydroxide (NaOH) were purchased from RFCL Ltd. (Mumbai, India) and methanol from S.D. Fine-Chem. Ltd. (Mumbai, India). 18 MΩ ultra pure water from Smart2Pure system (Thermo Electron LED GmbH, Germany) was used for preparing solutions and washing purposes.

2.2. Treatment of glass slides

To prepare the glass slides for thin film deposition, the microscope glass slides (Polar India Corporation, Mumbai) were cleaned by immersing them completely in 0.1 M HCl solution for an hour. The slides were then successively sonicated in water and methanol for 15 min each, followed by vacuum drying.

2.3. Sonochemical synthesis of γ-Fe_2O_3 nanoparticles

Sonochemical synthesis of γ-Fe_2O_3 nanoparticles was carried out using an ultrasound probe (BO3 Ultrasonic Processor UP1200, Cromtech, India). An excess of aqueous NaOH solution was added drop-wise to a 0.08 M aqueous solution of $FeCl_3$ under ultrasound [5,33]. The temperature of the reaction mixture was maintained at 30 ± 2 °C. A deep orange precipitate was obtained, which was centrifuged at 8000 rpm, washed with water and dried in air at 80 °C. The resulting reddish-brown powder was annealed at 500 °C for 2 h to obtain γ-Fe_2O_3.

2.4. Synthesis and in situ deposition of PANi/γ-Fe_2O_3 oxide nanocomposites

PANi/γ-Fe_2O_3 nanocomposites were prepared by chemical polymerization route. Aniline was dissolved in an aqueous solution mixture of 1 M $HClO_4$ and 0.05 M SDS by continuous stirring. Predetermined amount of ferric oxide nanoparticles were dispersed into the aniline solution via ultrasound. Two pretreated glass slides were placed in the beaker containing aniline solution. Polymerization of aniline was facilitated by drop-wise addition of aqueous solution of APS and 1 M $HClO_4$ under continuous stirring at ambient temperature (30 ± 1 °C). The molar ratio of APS to aniline was kept at 1.25. Following the addition of APS, the reaction mixture was stirred for an additional hour and then left to stand overnight. Thereafter, the glass slides were taken out of the reaction mixture at a retrieval speed of 0.1 mm/min. Dark green, uniform films of doped PANi/γFe_2O_3 were deposited on the glass slides; these were washed with water and methanol and vacuum dried for 30 min.

Different batches of PANi/γ-Fe_2O_3 nanocomposites were prepared wherein the amount of γ-Fe_2O_3 nanoparticles incorporated into PANi were varied as 1, 2 and 3 wt%, and subsequently labeled as F1, F2 and F3, respectively. Polyaniline doped with HCl and $HClO_4$/SDS system were prepared as control and labeled as PH and PHS, respectively.

2.5. Characterization

2.5.1. Fourier transform infrared (FTIR) spectroscopy

Fourier transform infrared (FTIR) spectra of pure PANi and its nanocomposites were recorded on Shimadzu FTIR-8400 spectrophotometer (Tokyo, Japan) within the wavenumber range of 400–4000 cm^{-1}. The samples were prepared in the pellet form by mixing with potassium bromide (KBr).

2.5.2. UV-visible spectroscopy

UV–vis absorption spectra of the samples dissolved in NMP (0.1 mg sample/25 mL NMP) were recorded on a Hitachi U-2900 spectrophotometer (Tokyo, Japan) in the range of 200–800 nm.

2.5.3. X-ray diffraction (XRD)

X-ray diffraction (XRD) analysis of γ-Fe_2O_3 and PANi/γ-Fe_2O_3 nanocomposites were conducted on Brukers D8 Advance X-ray diffractometer (Germany) with CuKα$_1$ radiation (λ = 1.5404 Å) within the 2θ range of 20–80°.

2.5.4. Field emission scanning electron microscopy (FE-SEM)

A Hitachi S-4800 field emission scanning electron microscope (Tokyo, Japan) was used to assess the surface morphology of thin films of PANi and its nanocomposites. The samples were given a gold coating and mounted on a specimen stub prior to viewing under the microscope.

2.5.5. Measurement of sensitivity of PANi/γFe_2O_3 nanocomposites to LPG at room temperature

Thin films of PANi (PH and PHS) and PANi/γ-Fe_2O_3 nanocomposites (F1, F2 and F3) were loaded in a sensing chamber and two conducting probes were placed in contact with the films. The current–voltage (*I–V*) characteristics of the thin films were recorded in the bias range of 2 to −2 V by a multi meter through the two probes. The *I–V* characteristics of each sample was recorded first in ambient air and then in different concentrations of commercial grade LPG gas (50, 100, 150 and 200 ppm) mixed with air. The electrical resistance of the films was deduced from *I–V* graphs; a change in electrical resistance gave the sensitivity of the films to LPG. The response of the sensor was measured after a fixed interval of 60 s. To determine the effect of humidity on the sensor response toward LPG, measurements were also taken at two different levels of relative humidity (RH) (∼22% and 67%). All the electrical measurements were taken at room temperature (30 ± 2 °C).

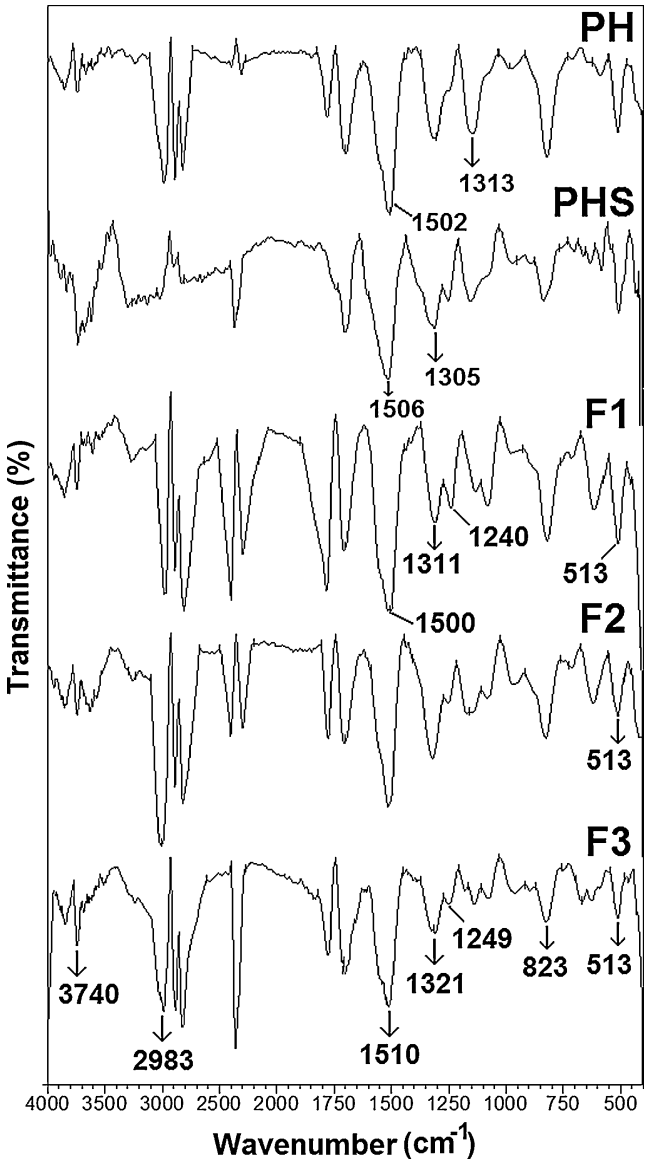

Fig. 1. FTIR spectra of PANi/HCl (PH), PANi/$HClO_4$-SDS (PHS) and PANi/γ-Fe_2O_3 nanocomposites at 1 wt% (F1), 2 wt% (F2) and 3 wt% (F3) γ-Fe_2O_3 content.

3. Results and discussion

3.1. Functional group identification by FTIR

Fig. 1 shows the characteristic functional groups of PANi. The main peaks observed in PH are 1502 and 1313 cm^{-1} corresponding to the quinoid and benzenoid ring stretching, which shows the aromatic structure of PANi. The peaks at 3740 and 2983 cm^{-1} are associated with – N—H and C—H stretching vibrations, respectively. The band at 1240 cm^{-1} can be assigned to bi-polaron structure related to C—N bond stretching of secondary aromatic amine, while the band at 823 cm^{-1} can be attributed to aromatic out-of-plane C—H bending. A thin film of PANi doped with HCl has the disadvantage of getting readily de-doped in air. To overcome this problem, PANi and its nanocomposites were doped with the binary dopant ($HClO_4$-SDS system), which extended their life in doped form (Fig. 2), and rendered them usable in sensors. In case of PHS, the quinoid and benzenoid rings appear at 1506 and 1305 cm^{-1}, respectively, indicating a structural change as a result of doping. The peak at 1240 cm^{-1} is more pronounced for PHS and the

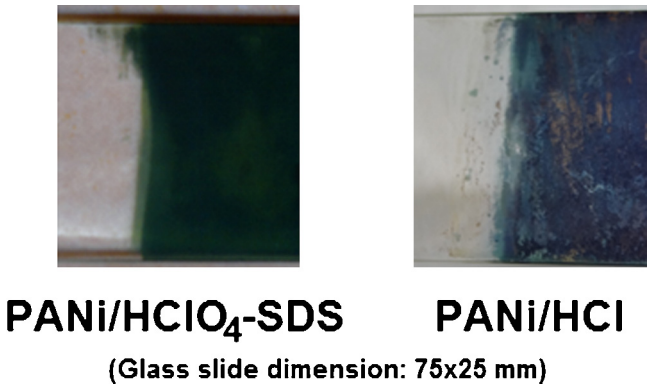

Fig. 2. In situ deposited thin films of PANi/$HClO_4$-SDS and PANi/HCl after air drying.

nanocomposites as compared to PH because the binary dopant causes a greater delocalization of electrons in PANi. The actual peak for Fe—O bond stretching is at ~553 cm^{-1} but it appears at 513 cm^{-1} in the nanocomposites [7]. The shift observed for this peak may be a result of the finite size of the particles and their interaction with PANi chains. A gradual shift in the absorbance peaks of the nanocomposites toward higher wavenumber is observed, corresponding to higher γ-Fe_2O_3 content. This is indicative of interaction between nano γ-Fe_2O_3 and PANi chain [34].

3.2. UV-visible spectroscopy

The UV–vis spectra (Fig. 3) show the characteristic peaks of polyaniline. In PHS the absorbance seen at 323 and 614 nm arises due to π–π^* and π–polaron transitions, respectively. In F1, F2 and F3, these peaks appear red-shifted to ~350 ± 5 nm and 620 ± 5 nm, respectively, as a result of interaction of γ-Fe_2O_3 nanoparticles with PANi chains. No obvious absorbance for the γ-Fe_2O_3 nanoparticles can be observed in the spectra. It is evident that PANi and its nanocomposites get de-doped when dissolved in NMP since the absorbance peaks belong to the emeraldine base form of PANi.

3.3. Phase identification by XRD

X-ray diffractograms of PANi and its nanocomposites are shown in Fig. 4. γ-Fe_2O_3 nanoparticles were characterized using XRD

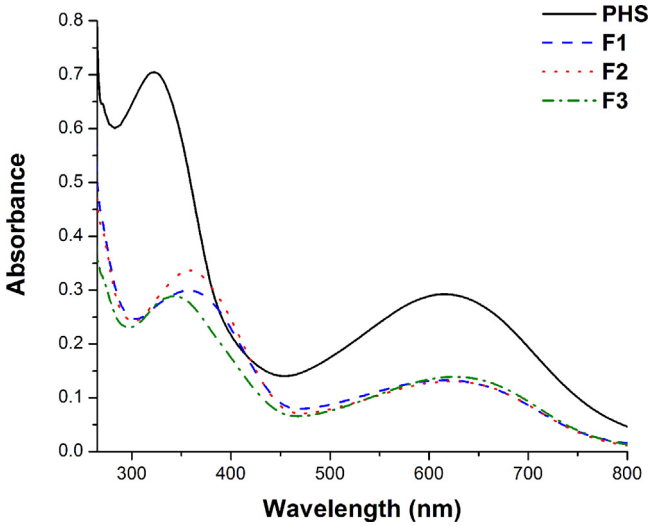

Fig. 3. UV–vis spectra of PANi/$HClO_4$-SDS (PHS), and PANi/γ-Fe_2O_3 nanocomposites at 1 wt% (F1), 2 wt% (F2) and 3 wt% (F3) γ-Fe_2O_3 content.

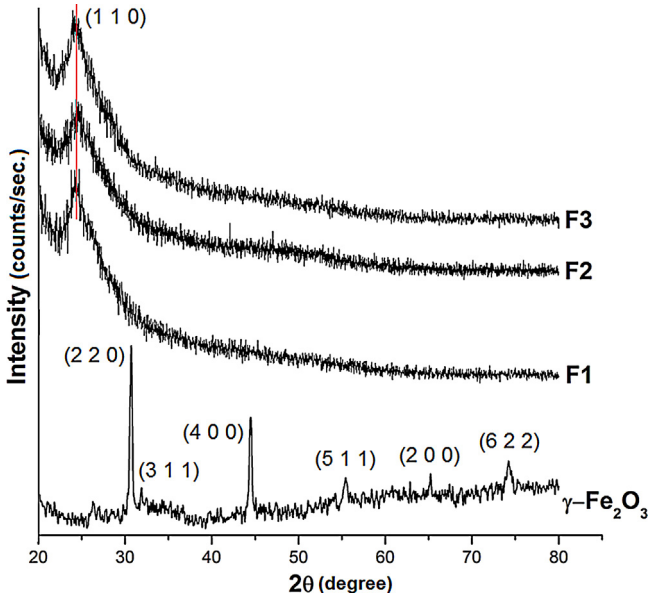

Fig. 4. X-ray diffraction patterns of γFe_2O_3 nanoparticles and PANi/γ-Fe_2O_3 nanocomposites at 1 wt% (F1), 2 wt% (F2) and 3 wt% (F3) γ-Fe_2O_3 content.

for phase identification before their incorporation into the PANi matrix. The observed peaks have *d*-values of 0.30, 0.27, 0.21, 0.16 and 0.12 nm corresponding to (2 2 0), (3 1 1), (4 0 0), (5 1 1) and (6 2 2) planes, respectively, which can be indexed to that of cubic γ-Fe_2O_3. The decreased relative intensity of (3 1 1) plane indicates changes in crystal structure [35]. The lattice constant for the γ-Fe_2O_3 nanoparticles, as calculated from XRD data, is found to be 0.823 nm, which has also been reported by Sahoo et al. [36]. Retama et al. [37] and Lindsley [38] observed this value as 0.835 nm, calculated through SAED. A minor peak corresponding to (2 0 0) plane is indicative of the presence of small amount of metallic iron; this shows a somewhat hybrid nature of the oxide. The crystallite size of these nanoparticles, as calculated by Scherrer's equation, is found to be 29.5 nm, and the crystallinity is ~55%. The XRD patterns of PANi/γ-Fe_2O_3 nanocomposites show a sharp peak at ~25°, which is associated with (1 1 0) plane of PANi. The crystallinity of F1 and F2 is about 63%, whereas for F3 it is 59%. The lowering of crystallinity could be due to higher γ-Fe_2O_3 content which hinders ordering of the polymer chain.

3.4. Surface morphology of thin films

Fig. 5(a–d) presents the FE-SEM micrographs of γ-Fe_2O_3 nanoparticles and PANi/γ-Fe_2O_3 nanocomposites (1, 2 and 3 wt%). Uniform, nanospheres of γ-Fe_2O_3 with a diameter of ~22 nm was observed in Fig. 5(a). This shows the effectiveness of ultrasound in producing non-aggregated nanoparticles even in the absence of an encapsulating agent. Fig. 5(b–d) shows the nanospheres of γ-Fe_2O_3 to be uniformly dispersed in the PANi matrix. Nanofibrillar morphology of polyaniline with a diameter of about 100, 96 and 70 nm (±5 nm) can be seen for F1, F2 and F3 systems, respectively. It appears that an increased amount of γ-Fe_2O_3 nanoparticles resulted in PANi nanofibers with smaller diameter. From the FE-SEM results it is evident that ultrasound induced cavitation produced non-aggregated, nanostructured γ-Fe_2O_3, and also aided in uniform dispersion of the nanoparticles into the polymer matrix.

3.4.1. Sensing of LPG by PANi/γ-Fe_2O_3 nanocomposites

The sensing of LPG in ambient conditions (in air) is a practical approach to observe sensor response to LPG in presence of atmospheric gases. Moreover, sensing at room temperature prevents response variation in sensor that typically results from high operating temperatures. It also facilitates safer detection of combustible gases like LPG. A pictorial representation of two-probe gas sensing setup is presented in Fig. 6. Fig. 7(a) shows the *I–V* curve of PH and PHS systems in air and at 200 ppm LPG. Semiconducting nature of PANi and its nanocomposites is evident from the non-linear *I–V* plot. PANi doped with the binary dopant (PHS) shows a much higher electrical conductivity as compared to conventional HCl doped PANi (PH). This could be because, unlike in PH, the binary dopant in PHS provides an effective electric route for the movement of charges which increases the electrical conductivity of PHS.

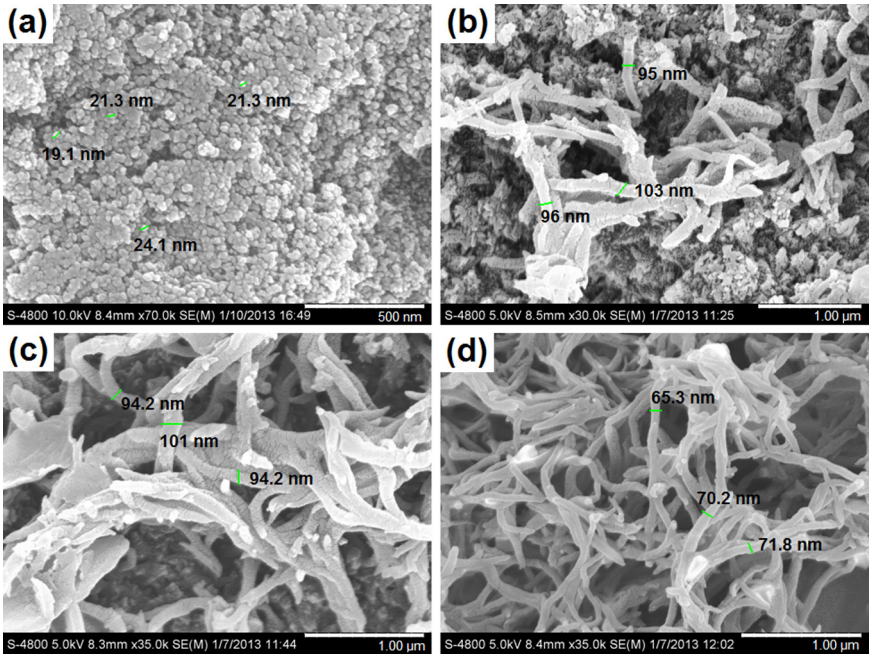

Fig. 5. FE-SEM micrographs of (a) γ-Fe_2O_3 nanoparticles (500 nm) and PANi/γ-Fe_2O_3 nanocomposites at 1 wt% (b), 2 wt% (c) and 3 wt% (d) (1 µm).

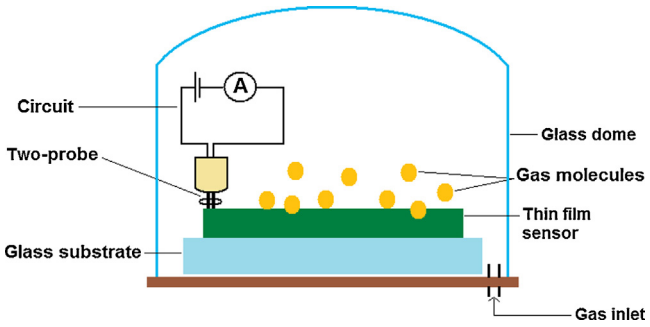

Fig. 6. Pictorial representation of a two-probe gas sensing setup.

No significant change in the electrical resistance of PH and PHS is observed on exposure to LPG. Thus, the introduction of the binary dopant only acts to increase the electrical conductivity and life of PANi in doped state but does not render it sensitive to LPG. However, with the incorporation of γ-Fe_2O_3 nanoparticles a pronounced increase in resistance is observed in the PANi/γ-Fe_2O_3 nanocomposite even when exposed to a low LPG concentration of 100 ppm, as shown in Fig. 7(b). This increase in resistance on exposure to LPG becomes more significant with increasing content of γ-Fe_2O_3

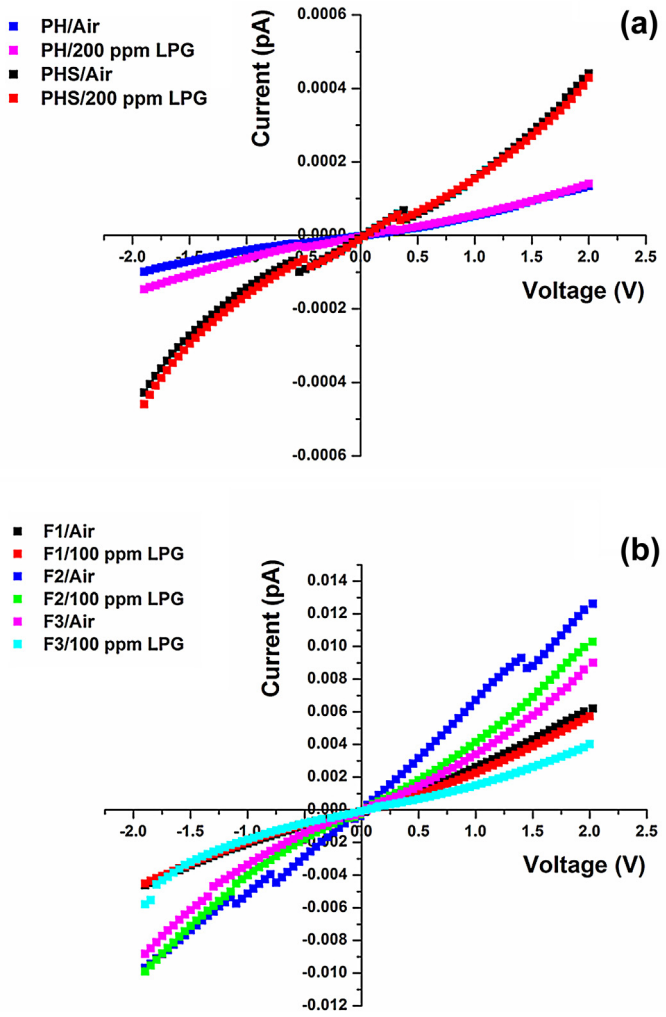

Fig. 7. (a) Current–voltage (*I–V*) curve of PANi/HCl (PH) and PANi/$HClO_4$-SDS (PHS) systems in air and at 200 ppm LPG. (b) Current–voltage (*I–V*) curve of PANi/γ-Fe_2O_3 nanocomposites at 1 wt% (F1), 2 wt% (F2) and 3 wt% (F3) γ-Fe_2O_3 content in air and at 100 ppm LPG.

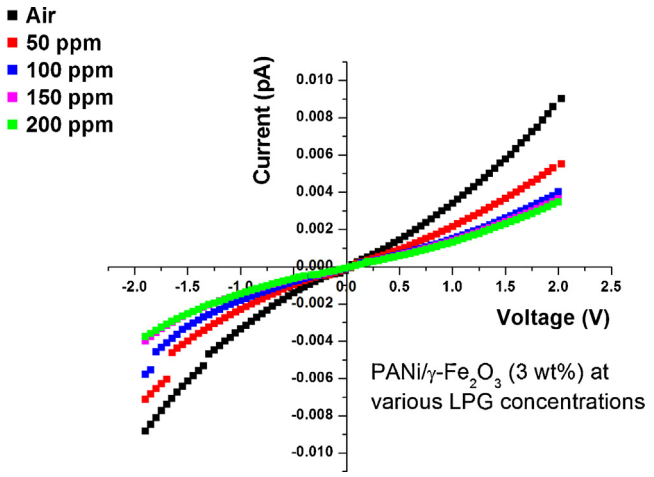

Fig. 8. Current–voltage (*I–V*) curve of PANi/γ-Fe_2O_3 nanocomposite at 3 wt% γ-Fe_2O_3 content (F3) in air and at different LPG concentrations.

nanoparticles. Fig. 8 shows *I–V* curve of F3 system in air and at LPG concentrations of 50–200 ppm. A significant increase in resistance is observed for F3 on exposure to a very low LPG concentration (50 ppm). Hence it is evident that a low amount of γ-Fe_2O_3 is sufficient in detection of LPG at concentrations much lower than its LFL. The increase in resistance is a result of change in electron density of the nanocomposite system upon exposure to LPG. In the PANi/γ-Fe_2O_3 nanocomposites, the p-type PANi combines with the n-type γ-Fe_2O_3 to form a hetero p-n junction with a depletion region. As the gas is injected into the sensing chamber, the gas molecules get adsorbed at the sensor surface and subsequently diffuse into the polymer where they interact with the polymer moieties. Such interaction induces a potential, which causes a change in the depletion region due to electron charge transfer and thus changes the resistance of the material [20,21,39,40]. The decrease in current, which is observed when the nanocomposite is exposed to LPG, indicates an increase in the depletion depth. Consequently, the size of the conducting channel within the nanocomposite decreases, and the resistance of the nanocomposite increases.

The sensor response to LPG was recorded using the fractional baseline manipulation method [41] that gives a normalized response, as shown in Eq. (1).

$$\text{Response} = \frac{R_g - R_a}{R_a} \quad (1)$$

In this equation, R_g is the resistance of sensor in presence of gas and R_a is the resistance of sensor in air. Fig. 9 shows the response v/s concentration graph of PANi/γ-Fe_2O_3 nanocomposites. It is observed that the response of the sensor increases with increase in amount of γ-Fe_2O_3 nanoparticles incorporated into PANi. Since the gas response of a sensor mainly depends on the surface interactions between the gas and the sensing material, therefore a greater surface area of the sensor leads to stronger interactions between the adsorbed gases and the sensor surfaces [42]. Consequently, an enhancement in gas response of the sensor is observed. In case of PANi/γ-Fe_2O_3 nanocomposite sensors, an increasing content of γ-Fe_2O_3 nanoparticles, due to their high surface area, increases the adsorption sites for the gas molecules leading to greater interaction between the gas and the sensor. Therefore at higher gas concentrations more of the gas molecules get adsorbed on the nanoparticle surface bringing about a change in the depletion region and increasing the resistance in a short time. The F3 sample thus shows a maximum response factor of 1.3 for 200 ppm LPG concentration. Even at 50 ppm LPG concentration, the response factor of F3 at 0.5 is much greater than that of F1 and F2 at a low response time of 60 s.

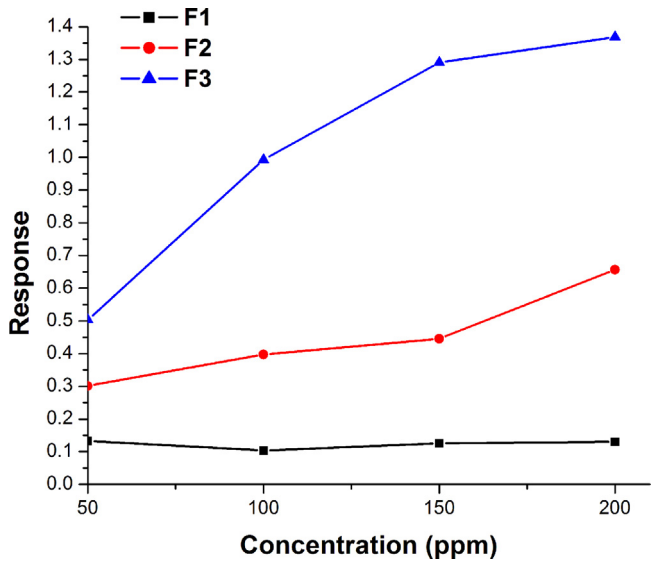

Fig. 9. Response v/s concentration graph of PANi/γ-Fe_2O_3 nanocomposites at 1 wt% (F1), 2 wt% (F2) and 3 wt% (F3) γ-Fe_2O_3 content.

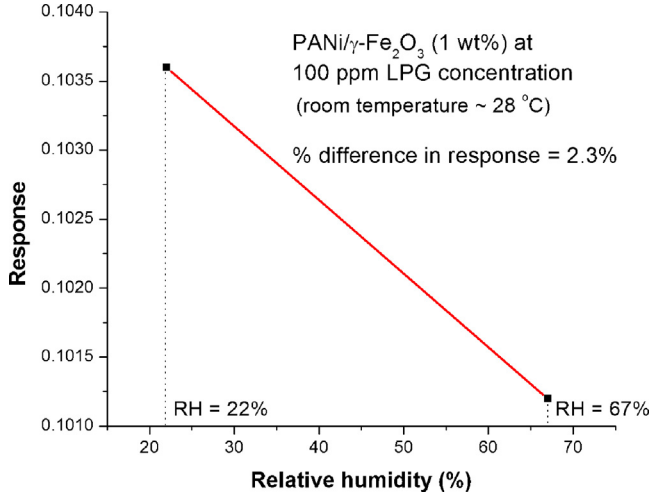

Fig. 10. Response v/s relative humidity graph of PANi/γ-Fe_2O_3 nanocomposites at 1 wt% γ-Fe_2O_3 content (F1) for 100 ppm LPG concentration.

Finally, to ascertain whether humidity affects the sensor response toward LPG, measurements were taken at relative humidity levels of 22% and 67% (room temperature ~28 °C). Fig. 10 shows the response v/s relative humidity plot of F1 for 100 ppm LPG at room temperature. A minor decrease in sensor response was observed for an increase in humidity level, the percentage difference in response between the two humidity levels being 2.3%. This results from polarization of water molecules near the PANi surface, which leads to formation of attractive forces between water molecules and the polymer. A thin layer of water thus forms on the PANi surface, which decreases the number of adsorbed gas molecules resulting in lowering of response [43].

4. Conclusion

PANi and PANi/γ-Fe_2O_3 nanocomposites were chemically synthesized at room temperature using a novel binary dopant, and their films were deposited in situ on glass substrates. The PANi/binary dopant system did not get de-doped in air, thus facilitating its use as a sensing layer. To induce sensitivity, sonochemically synthesized γ-Fe_2O_3 nanoparticles were incorporated into the PANi matrix in varied amounts (1–3 wt%). Spherical nanoparticles of γ-Fe_2O_3 having an average size of ~22 nm were found to be embedded into nanofibrillar PANi. These nanocomposite films were tested for LPG sensing at room temperature. The interaction between the gas molecules and the nanocomposite material induces a potential causing an increase in the depletion area of PANi/γ-Fe_2O_3. As a result, the resistance of the material increases upon exposure to LPG. The sensor response toward LPG increased with increasing amount of γ-Fe_2O_3 nanoparticles in the nanocomposite. The large surface area of γ-Fe_2O_3 nanoparticles provided greater adsorption sites for the gas molecules. This resulted in higher response at higher γ-Fe_2O_3 content. PANi/γ-Fe_2O_3 (3 wt%) nanocomposite exhibited excellent gas response at a low gas concentration of 50 ppm with a response time of 60 s. A slight lowering of sensor response toward LPG was observed at a higher relative humidity level.

Acknowledgement

One of the authors (T. Sen) is thankful to the University Grants Commission, New Delhi, India for providing financial support under the RFSMS scheme.

References

[1] V.K. Rana, A.K. Pandey, R.P. Singh, B. Kumar, S. Mishra, C.S. Ha, Enhancement of thermal stability and phase relaxation behavior of chitosan dissolved in aqueous L-lactic acid: using 'silver nanoparticles' as nano filler, Macromol. Res. 18 (2010) 713–720.
[2] S. Mishra, N.G. Shimpi, A.D. Mali, Influence of nano inorganic particles on properties of epoxy nanocomposites, Polym. Plast. Technol. Eng. 50 (2011) 758–761.
[3] S. Mishra, N.G. Shimpi, A.D. Mali, Investigation of photo-oxidative effect on morphology and degradation of mechanical and physical properties of nano $CaCO_3$ silicone rubber composites, Polym. Adv. Technol. (2011), http://dx.doi.org/10.1002/pat.1861.
[4] S. Jing, S. Xing, L. Yu, Y. Wu, C. Zhao, Synthesis and characterization of Ag/polyaniline core–shell nanocomposites based on silver nanoparticles colloid, Mater. Lett. 61 (2007) 2794–2797.
[5] S. Mishra, N.G. Shimpi, T. Sen, The effect of PEG encapsulated silver nanoparticles on the thermal and electrical property of sonochemically synthesized polyaniline/silver nanocomposite, J. Polym. Res. 20 (2013) 49–58.
[6] B. David, O. Schneeweiss, E. Santava, O. Jasek, Magnetic properties of γ-Fe_2O_3 nanopowder synthesized by atmospheric microwave torch discharge, Acta Phys. Polon. A. 122 (2012) 9–11.
[7] S.K. Apte, S.D. Naik, R.S. Sonawane, B.B. Kale, J.O. Baeg, Synthesis of nanosize-necked structure α- and γ-Fe_2O_3 and its photocatalytic activity, J. Am. Ceram. Soc. 90 (2007) 412–414.
[8] B.B. Li, M.R. Ji, X.M. Ni, F. Zhou, D.E. Zhang, J. Cheng, Convenient approach to γ-Fe_2O_3 nanoparticles: magnetic and electrochemical properties, Chin. J. Chem. Phys. 20 (2007) 203.
[9] M.S. Islam, J. Kurawaki, Y. Kusumoto, M. Abdulla-Al-Mamun, M.Z. Bin Mukhlish, Hydrothermal novel synthesis of neck-structured hyperthermia-suitable magnetic (Fe_3O_4, γ-Fe_2O_3 and α-Fe_2O_3) nanoparticles, J. Sci. Res. 4 (2012) 99–107.
[10] V. Sreeja, P.A. Joy, Microwave-hydrothermal synthesis of γ-Fe_2O_3 nanoparticles and their magnetic properties, Mater. Res. Bull. 42 (2007) 1570–1576.
[11] R. Strobel, S.E. Pratsinis, Direct synthesis of maghemite, magnetite and wustite nanoparticles by flame spray pyrolysis, Adv. Powder Technol. 20 (2009) 190–194.
[12] X.M. Liu, S.Y. Fu, H.M. Xiao, Synthesis of maghemite sub-microspheres by simple solvothermal reduction method, J. Solid State Chem. 179 (2006) 1554–1558.
[13] Z. Jing, S. Wu, Synthesis, characterization and gas sensing properties of undoped and Co-doped γ-Fe_2O_3-based gas sensors, Mater. Lett. 60 (2006) 952–956.
[14] Z. Jing, Y. Wang, S. Wu, Preparation and gas sensing properties of pure and doped γ-Fe_2O_3 by an anhydrous solvent method, Sens. Actuators B 113 (2006) 177–181.
[15] A.K. Dutta, S.K. Maji, D.N. Srivastava, A. Mondal, P. Biswas, P. Paul, B. Adhikary, Peroxidase-like activity and amperometric sensing of hydrogen peroxide by Fe_2O_3 and Prussian blue-modified Fe_2O_3 nanoparticles, J. Mol. Catal. A: Chem. 360 (2012) 71–77.
[16] S. Agarwala, Z.H. Lim, E. Nicholson, G.W. Ho, Probing the morphology-device relation of Fe_2O_3 nanostructures towards photovoltaic and sensing applications, Nanoscale 4 (2012) 194–205.
[17] G. Fan, Y. Wang, M. Hu, Z. Luo, K. Zhang, G. Li, Template free synthesis of hollow ball-like nano-Fe_2O_3 and its application to the detection of dimethyl methylphosphonate at room temperature, Sensors 12 (2012) 4594–4604.
[18] L. Liao, Z. Zheng, B. Yan, J.X. Zhang, H. Gong, J.C. Li, C. Liu, Z.X. Shen, T. Yu, Morphology controllable synthesis of α-Fe_2O_3 1D nanostructures: growth

mechanism and nanodevice based on single nanowire, J. Phys. Chem. C 112 (2008) 10784–10788.
[19] S. Si, C. Li, X. Wang, Q. Peng, Y. Li, Fe_2O_3/ZnO core–shell nanorods for gas sensors, Sens. Actuators B 119 (2006) 52–56.
[20] D. Yang, Nanocomposite films for gas sensing, in: B. Reddy (Ed.), Advances in Nanocomposites – Synthesis, Characterization and Industrial Applications, In Tech, Croatia, 2011, pp. 857–882.
[21] S.S. Joshi, C.D. Lokhande, S.H. Han, A room temperature liquefied petroleum gas sensor based on all-electrodeposited n-CdSe/p-polyaniline junction, Sens. Actuators B 123 (2007) 240–245.
[22] S.A. Waghuley, S.M. Yenorkar, S.S. Yawale, S.P. Yawale, Application of chemically synthesized conducting polymer-polypyrrole as a carbon dioxide gas sensor, Sens. Actuators B 128 (2008) 366–373.
[23] V.C. Goncalves, D.T. Balogh, Optical VOCs detection using poly(3-alkylthiophenes) with different side-chain lengths, Sens. Actuators B 142 (2009) 55–60.
[24] D.S. Sutar, N. Padma, D.K. Aswal, S.K. Deshpande, S.K. Gupta, J.V. Yakhmi, Preparation of nanofibrous polyaniline films and their application as ammonia gas sensor, Sens. Actuators B 128 (2007) 286–292.
[25] Z. Jin, Y. Su, Y. Duan, Development of a polyaniline-based optical ammonia sensor, Sens. Actuators B 72 (2001) 75–79.
[26] P. Stamenov, R. Madathil, J.M.D. Coey, Dynamic response of ammonia sensors constructed from polyaniline nanofibre films with varying morphology, Sens. Actuators B 161 (2012) 989–999.
[27] S. Sharma, C. Nirkhe, S. Pethkar, A.A. Athawale, Chloroform vapour sensor based on copper/polyaniline nanocomposite, Sens. Actuators B 85 (2002) 131–136.
[28] J. Zheng, G. Li, X. Ma, Y. Wang, G. Wu, Y. Cheng, Polyaniline-TiO_2 nanocomposite-based trimethylamine QCM sensor and its thermal behavior studies, Sens. Actuators B 133 (2008) 374–380.
[29] Y. Sun, G. Guo, B. Yang, W. Cai, Y. Tian, M. He, Y. Liu, One-step solution synthesis of Fe_2O_3 nanoparticles at low temperature, Physica B 406 (2011) 1013–1016.
[30] Z. Wang, H. Bi, J. Liu, T. Sun, X. Wu, Magnetic and microwave absorbing properties of polyaniline/γ-Fe_2O_3 nanocomposite, J. Magn. Magn. Mater. 320 (2008) 2132–2139.
[31] K. Singh, A. Ohlan, R.K. Kotnala, A.K. Bakhshi, S.K. Dhawan, Dielectric and magnetic properties of conducting ferromagnetic composite of polyaniline with γ-Fe_2O_3 nanoparticles, Mater. Chem. Phys. 112 (2008) 651–658.
[32] T.F. Barry, Application of fire and explosion risk assessment to an LPG bulk storage facility, in: M.M. Hirschler (Ed.), Fire Hazard and Fire Risk Assessment, ASTM STP 1150, Philadelphia, 1992, pp. 183–206.
[33] S. Sonawane, P. Chaudhari, S. Ghodke, S. Ambade, S. Gulig, A. Mirikar, A. Bane, Combined effect of ultrasound and nanoclay on adsorption of phenol, Ultrason. Sonochem. 15 (2008) 1033–1037.
[34] H. Gu, Y. Huang, X. Zhang, Q. Wang, J. Zhu, L. Shao, N. Haldolaarachchige, D.P. Young, S. Wei, Z. Guo, Magnetoresistive polyaniline-magnetite nanocomposites with negative dielectrical properties, Polymer 53 (2012) 801–809.
[35] M. Pal, A. De, Polymer-iron oxide based magnetic nanocomposites, in: L. Merhari (Ed.), Hybrid Nanocomposites for Nanotechnology: Electronic, Optical, Magnetic and Biomedical Applications, Springer Science+Business Media, New York, 2009, pp. 454–506.
[36] S.K. Sahoo, K. Agarwal, A.K. Singh, B.G. Polke, K.C. Raha, Characterization of γ- and α-Fe_2O_3 nano powders synthesized by emulsion precipitation-calcination route and rheological behaviour of α-Fe_2O_3, Int. J. Eng. Sci. Technol. 2 (2010) 118–126.
[37] J. Rubio-Retama, N.E. Zafeiropoulos, C. Serafinelli, R. Rojas-Reyna, B. Voit, E.L. Cabarcos, M. Stamm, Synthesis, Characterization of thermosensitive PNIPAM microgels covered with superparamagnetic γ-Fe_2O_3 nanoparticles, Langmuir 23 (2007) 10280–10285.
[38] D. Lindsley, Experimental studies of oxide minerals, in: D. Rumble III (Ed.), Reviews in Minerology, Minerological Society of America, Washington, DC, 1976, L-18.
[39] D.S. Dhawale, D.P. Dubal, A.M. More, T.P. Gujar, C.D. Lokhande, Room temperature liquefied petroleum gas (LPG) sensor, Sens. Actuators B 147 (2010) 188–191.
[40] A. Parveen, A. Koppalkar, A.S. Roy, Liquefied petroleum gas sensing of polyaniline-titanium dioxide nanocomposites, Sens. Lett. 11 (2013) 242–248.
[41] K. Arshak, E. Moore, G.M. Lyons, J. Harris, S. Clifford, A review of gas sensors employed in electronic nose applications, Sens. Rev. 24 (2004) 181–198.
[42] S. Chaisitsak, Nanocrystalline SnO_2:F thin films for liquid petroleum gas sensors, Sensors 11 (2011) 7127–7140.
[43] M.E. Azim-Araghi, M.J. Jafari, Electrical and gas sensing properties polyaniline chloroaluminium phthalocyanine composite thin films, Eur. Phys. J. Appl. Phys. 52 (2010) 10402–10407.

Biographies

Tanushree Sen obtained her M.Sc. in 2006 in Polymer Science. She is presently pursuing Ph.D. from University Institute of Chemical Technology, North Maharashtra University, Jalgaon, Maharashtra, India. Her areas of research are intrinsically conducting polymers, gas sensors, fiber reinforced plastics, and polymeric blends and alloys.

N.G. Shimpi completed his Ph.D. in 2006. He is presently assistant professor and in-charge head of Department of Nano Science and Technology at University Institute of Chemical Technology, North Maharashtra University, Jalgaon. He has 37 published research papers in various international and national journals. He has a research experience of 9 years on areas such as polymer nano composites, rubber composites and nano-fillers.

Satyendra Mishra did his Ph.D. from Indian Institute of Technology, Delhi in 1989. He is presently the director of UICT, NMU, Jalgaon, Maharashtra. He has been continually engaged in research activities for the last 30 years. He has over 140 published research papers in various international and national journals. His areas of research are polymer nano composites, water soluble polymers, wood polymer composites, nano-polymers, reaction engineering aspects of depolymerization reactions, nano catalysis and gas sensors.

Ramphal Sharma did his Ph.D. from University of Rajasthan, Jaipur in 1991. He is presently an associate professor at the Department of Physics, Dr. B.A.M. University, Aurangabad, Maharashtra. He has 23 years of experience in research and development in solid state physics, thin film semiconductors and nanotechnology.